A Sensitive Spectral Survey of Interstellar Features in the Near-UV [3040-3700Å]

N. H. Bhatt[1] and J. Cami[1,2]

[1] Department of Physics and Astronomy, University of Western Ontario,
London, ON N6A 3K7, Canada
email: nbhatt3@uwo.ca

[2]SETI Institute, 189 Bernardo Avenue, Suite 100, Mountain View, CA 94043, USA

Abstract. We present a comprehensive and sensitive unbiased survey of interstellar features in the near-UV range (3040-3700 Å). We combined a large number of VLT/UVES archival observations of a sample of highly reddened early type stars – typical diffuse interstellar band (DIB) targets. We stacked the individual observations to obtain a spectrum with a signal-to-noise ratio exceeding 1500. Careful inspection of this spectrum reveals tens of absorption features of interstellar nature, most of which can be identified with various atomic and molecular features. We furthermore detect four weak unidentified features, but we cannot establish their interstellar nature. Our sensitivity is limited by telluric and instrumental residuals; this precludes us from detecting broader features (e.g. DIBs). For each detected feature, we measured fundamental parameters (radial velocities, line widths, and equivalent widths). We also compare our co-added spectrum to cold gas-phase laboratory measurements of small, neutral polycyclic aromatic hydrocarbon (PAH) molecules.

**Keywords.** ISM: atoms, ISM: molecules, ISM: lines and bands

1. Introduction

Various multi-wavelength studies (optical, IR, UV) have revealed a rich chemical diversity in the interstellar medium (see e.g. Herbst & van Dishoeck 2009; Tielens 2013, for reviews). In addition to the more than 100 identified atomic and molecular species (Savage & Sembach 1996; Tielens 2013), hundreds of DIBs have been detected, indicating the presence of many more stable and abundant chemical compounds in space (Herbig 1995, see also Snow, this volume). To date, there has not been a conclusive identification of a DIB carrier.

Electronic transitions of some promising DIB carriers (e.g. C_{60}, small neutral PAHs) occur in the relatively unexplored near-UV wavelength range (3100-3700 Å). Observations in this range have been hampered largely by the lack of instruments with sufficient sensitivity in this range and by strong telluric contamination. Nevertheless, Salama *et al.* (2011) and Gredel *et al.* (2011) carried out searches for the transitions of specific PAHs in near-UV spectroscopic observations. In both cases, no interstellar PAH absorption bands were detected; however, Gredel *et al.* (2011) detected some interstellar lines originating from OH^+, NH, CH, CH^+ and CN in this wavelength range.

To the best of our knowledge, a survey of the entire near-UV range has not been carried out. Here, we present preliminary results of a sensitive and unbiased survey of interstellar features in the near-UV. Section 2 describes our data set of archival VLT/UVES observations, data processing and analysis methods. We discuss our results in Section 3.
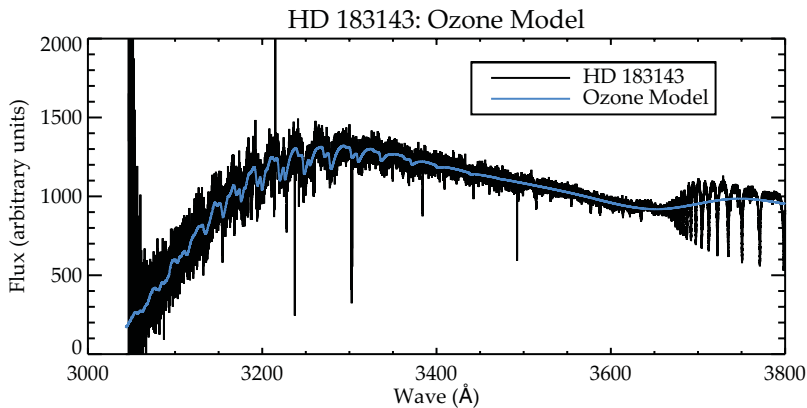
Figure 1. The fully reduced UVES spectrum (346 setting) for HD 183143 (black), and our best-fit model for telluric ozone (blue).

## 2. Targets, Observations and Methods

2.1. *Observations*

The survey described in this paper requires detecting often weak, and generally fairly narrow lines. Very few instruments have the proper combination of resolving power and sensitivity in the near-UV to achieve this task. The UVES échelle spectrograph (Dekker *et al.* 2000) mounted on the VLT, is ideally suited for our purposes. UVES is capable of measuring from 3000–11000Å at a resolving power of 80,000 or more. Here, we use in particular the standard 346 setting which covers the range 3030–3880Å.

Our study is entirely based on ESO archival observations. Since our aim is to detect interstellar features (both weak and strong), we have selected targets which trace a significant quantity of interstellar material (i.e. highly reddened stars as measured through their $E(B-V)$); have sufficient near-UV flux and a minimal amount of stellar lines (i.e. early-type stars). We have additionally also included a few single cloud lines of sight. Thus, our data set includes many typical and ideal DIB targets. Our final data set consists of 185 spectra corresponding to 51 reddened targets.

2.2. *Data Processing*

For many observations, fully reprocessed data products are available from the ESO archive; we have used these where available. For other observations, we used the standard UVES pipeline recipe to reduce the data with Gasgano. At this point, the quality of the reduced spectra reflect the difficulties in observing in this range: the signal-to-noise (S/N) ratio for a single observation varies across the spectrum, but is typically low ($\sim$40), and reaches a minimum at the shortest wavelengths ($\sim$3030Å). We next clean our spectra from bad pixels and cosmic rays.

As can be seen from Fig. 1, the near-UV is affected by strong telluric ozone absorption in the Huggins band, occurring between $\sim$3000-3400Å. To correct for these spectral features, we modeled the spectral dependence of the ozone absorption bands for each observation independently using the cross sections from Burrows *et al.* (1999), and varying the optical depth to achieve the best fit to the observations. An example of the best-fit ozone model can be seen in Fig. 1; we then divided the spectra by this model. Note that
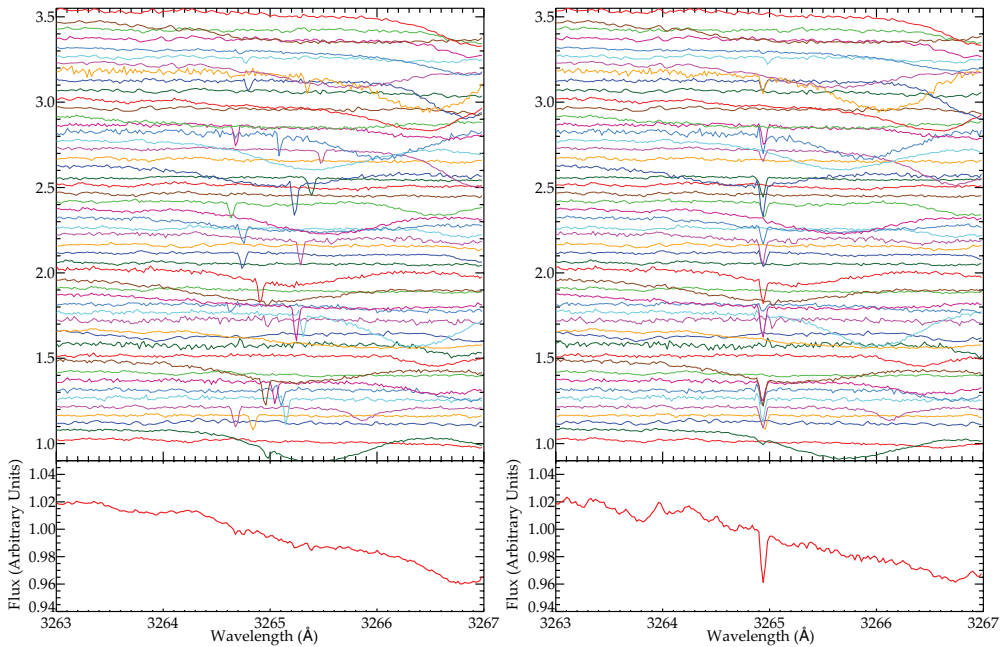
Figure 2. Optimal spectra for all our targets in the *interstellar* rest frame (left), and in the *geocentric* rest frame (right). The corresponding superspectra are shown at the bottom. While weak and narrow features appear in the interstellar superspectrum, this comparison clearly shows they originate from telluric residuals.

this does not remove all telluric features – only the fairly broad ozone bands. Many (narrow) remaining atmospheric features are present in the spectra; when comparing spectra in the geocentric frame, the telluric nature of these features becomes obvious.

We then determined the continuum in our spectra by fitting a cubic spline through well-selected anchor points, and normalized our spectra. For each observations, we applied a heliocentric correction. Finally, we co-added the relevant observations to create an *optimal spectrum* for each of the 51 targets. These optimal spectra are obtained by calculating the weighted mean flux of each observation at each wavelength, with weights determined by the exposure time. The resulting optimal spectra typically have a S/N of ∼250.

2.3. *Searching for Interstellar Features*

It is then convenient to create three different co-adds that include *all* our observations – so-called *superspectra*. In all three cases, we first shift the spectra to a specific rest frame – geocentric, stellar or interstellar – before co-adding all observations. Interstellar velocities were derived from the central wavelength of the observed Na I doublet at 3302Å. We determined stellar velocities from a cross-correlation with a model containing H and He lines; these values generally correspond very well to values found in the literature. The resulting superspectra furthermore have a S/N exceeding 1500, and thus allow a more sensitive search than would be possible in the individual target spectra.

We then identify interstellar features by visually searching for absorption features in these superspectra. We expect that a feature should appear most well defined in its intrinsic frame. For example, a known interstellar line should appear strong and narrow

Table 1. Identification and wavelengths of all 31 interstellar features (originating from 11 different atomic and molecular species) that were detected in our spectra.

Species	Wavelength (Å, air)
Cr I	3578.683, 3593.482
Fe I	3440.606, 3679.913
K I	3217.154
Na I	3302.368, 3302.987
Ti II	3066.354, 3072.984, 3229.199, 3241.994, 3383.768
CH	3137.530, 3143.150, 3146.010, 3627.403, 3633.289, 3636.222
CH^+	3447.075, 3579.020
CN	3579.453, 3579.963, 3580.937
NH	3353.924, 3358.053
OH	3072.010, 3072.064, 3078.440, 3078.472, 3081.664
OH^+	3583.769

in the interstellar rest frame because the feature systematically aligns in the the optimal interstellar rest frame spectra. This same paradigm allows us to detect and recognize residual atmospheric features (see e.g. Fig. 2).

3. Results

From a careful visual search and comparison between the three different superspectra, we initially marked a total of ∼100 absorption features as possible interstellar features. While most of those (∼70 features) turn out to be due to telluric residuals or artefacts, 12 can be firmly identified with atomic absorption lines and 19 more with various molecular lines (see Table 1) that all have been detected previously in some interstellar lines of sight. Our method is thus indeed sensitive to detect interstellar lines. Four more weak features appear in the interstellar superspectrum (at 3144.705Å, 3346.968Å, 3362.942Å and 3572.656Å) for which we have not been able to find an identification in the literature. The first three only show up in the superspectrum, but not in the individual target optimal spectra; these may thus be at our detection limit. As an additional test for the interstellar nature of the remaining feature at 3572.656Å, we measured the equivalent width of this line in the optimal spectra of each target; we would then expect that an interstellar feature would show stronger absorption for more reddened targets. However, no such trend is found (Fig. 3), and thus it is unlikely that this feature is interstellar, especially given the large range in $E(B-V)$ of our targets. Note though that our measurements indicate only a marginal detection in the optimal spectra.

Apart from the 31 known atomic and molecular lines, we have thus detected no other feature that is clearly of interstellar origin. This indicates that there are at best very few unknown interstellar lines in the near-UV range. However, we must point out several caveats. First of all, it is clear that our sensitivity is limited by the presence of many telluric residuals. Indeed, the measured S/N in the geocentric superspectrum is much lower than in the interstellar superspectrum. In the latter, the telluric residuals largely cancel out due to Doppler shifts, but in a few occasions, they conspire to cause weak features in the interstellar superspectrum (see e.g. Fig 2). In practice, we found that we can probably detect features if they are at about the 8σ level in the interstellar super-spectrum. For the narrowest features that we could detect (with a FWHM of ∼45mÅ), our detection limit is thus ∼ 0.3 mÅ. Second, when features are too broad, our method does not provide enough pairwise contrast between the superspectra to recognize interstellar lines. From simulations, we have found that the broadest feature that we could
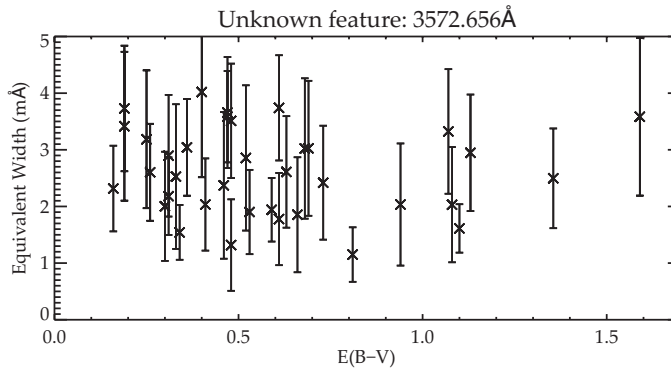
Figure 3. The equivalent width for the weak, unidentified feature at 3572.656Å measured in all our optimal spectra, as a function of $E(B-V)$. No increase with $E(B-V)$ is noted, and in fact, all measurements are near the detection limit. This feature is thus likely an artefact.

reliably recognize in the superspectra has a FWHM of 0.8Å, if it has a depth of at least 0.5% (or thus an equivalent width of at least 6 mÅ). With these sensitivities, we can then also determine upper limits of the order of $N \leqslant 10^{12}$ cm^{-2} to the column densities of several PAH species (e.g. benzo[ghi]perylene, pyrene), following the same approach as described in Salama *et al.* (2011) and Gredel *et al.* (2011) and using the same oscillator strengths. However, since these upper limits are derived from the (averaged) interstellar superspectrum, they are only indicative.

4. Summary & Conclusions

We have carried out a sensitive search for narrow, interstellar features in the near-UV between 3040–3700Å by combining a large number of observations and using different reference frames. We have detected 31 known interstellar lines (atomic and molecular) in this range, and find 2 lines that are possibly interstellar. Our sensitive is limited by many telluric features, and by instrumental issues that do not allow us to detect DIBs broader than 0.8Å.

Acknowledgements

References

Burrows J. P., Richter A., Dehn A., *et al.*1999, *J. Quant. Spectrosc. Radiat. Transfer* 61, 509

Dekker H., D'Odorico S., Kaufer A., Delabre B., & Kotzlowski H. 2000, In: Iye M., Moorwood A. F. (eds.), *Optical and IR Telescope Instrumentation and Detectors*, vol. 4008 of *SPIE Conference Series*, pp. 534–545

Gredel R., Carpentier Y., Rouillé G., *et al.*2011, *A&A* 530, A26

Herbig G. H. 1995, *ARA&A* 33, 19

Herbst E. & van Dishoeck E. F. 2009, *ARA&A* 47, 427

Salama F., Galazutdinov G. A., Krełowski J., *et al.*2011, *ApJ* 728, 154

Savage B. D. & Sembach K. R. 1996, *ARA&A* 34, 279

Tielens A. G. G. M. 2013, *Reviews of Modern Physics* 85, 1021

Discussion

ROUEFF: Did you detect isotopic species? In particular, $C_{13}H$, and $C_{13}H^+$?

BHATT: Despite our high signal-to-noise, we did not detect these.

MULAS: How did you determine which interstellar line to use to determine your interstellar velocity?

BHATT: We chose a line that was easily identifiable, and visible in all our targets. Therefore the Na I doublet was an ideal choice. We chose the main cloud velocity. This proved to be a reasonable choice since upon shifting to the interstellar restframe, many other interstellar lines appeared at exactly their rest wavelength.

GEBALLE : What are your plans for further investigations?

BHATT: It would be beneficial to deal with the stellar lines. This might be possible by adding spectroscopic binaries to the dataset.